Received Date : 12-Aug-2018

Revised Date : 18-Mar-2019

Accepted Date : 29-Apr-2019

Hyaluronan preconditioning of monocytes/macrophages affects their angiogenic behavior and regulation of TSG-6 expression in a tumor type-specific manner.

Fiorella M. Spinelli[a], Daiana L. Vitale[a], Antonella Icardi[a], Ilaria Caon[b], Alejandra Brandone[c], Paula Giannoni[d], Virginia Saturno[c], Alberto Passi[b], Mariana García[e], Ina Sevic[a], Laura Alaniz[a]✉.

[a]Laboratorio de Microambiente Tumoral, Centro de Investigaciones Básicas y Aplicadas (CIBA), Universidad Nacional de la Pcia. de Bs. As. Centro de Investigaciones y Transferencia del Noroeste de la Pcia. de Bs. As. (CIT NOBA, UNNOBA-CONICET), Junín, Bs. As., Argentina.

[b]Dipartimento di Medicina e Chirurgia, Università degli Studi dell'Insubria, Varese, Italia

[c]Hospital Interzonal General de Agudos Dr. Abraham F. Piñeyro, Junín, Bs. As., Argentina.

[d]Clínica Centro, Junín, Bs. As., Argentina.

[e]Laboratorio de Terapia Génica, IIMT – CONICET, Universidad Austral, Derqui-Pilar, Bs. As., Argentina.

Corresponding author

✉ Laura, Alaniz, PhD. Independent researcher from CONICET. Laboratorio de Microambiente Tumoral, Centro de Investigaciones Básicas y Aplicadas (CIBA), UNNOBA; CIT NOBA, (UNNOBA-CONICET). Jorge Newbery 261, Junín (B6000), BA, Argentina. Tel.: +54-236-4-407750 ext 11620

email: ldalaniz@comunidad.unnoba.edu.ar

Running title

HA action on Mo/MØ: tumor angiogenesis and TSG-6.

Article type : Original Article

Abbreviations

HA: hyaluronan
CM: conditioned media
MCM: MDA-MB-231 conditioned media
LCM: LoVo conditioned media
HMW: high molecular weight
LMW: low molecular weight
TL: tumor cell lysate
MTL: MDA-MB 231 tumor cell lysate
LTL: LoVo tumor cell lysate
TTL: tumor tissue lysate
NATL: normal tissue adjacent to the tumor lysate
Mo: monocytes
MØ: macrophages
TSG-6: tumor necrosis factor (TNF)-stimulated gene 6
PBMCs: peripheral blood mononuclear cells
ECs: endothelial cells
NRQ: normalized relative quantities

Keywords

Hyaluronan, TSG-6, monocytes/macrophages, angiogenesis, breast carcinoma, colorectal carcinoma.

Conflicts of Interest

The authors declare no conflict of interest.

Abstract

Hyaluronan is a glycosaminoglycan normally present in the extracellular matrix in most tissues. Hyaluronan is a crucial player in many processes associated with cancer, such as angiogenesis, invasion and metastasis. However, little has been reported regarding the action of hyaluronan on monocytes/macrophages in tumor angiogenesis and its consequences on tumor development. In the present study, we investigated the effects of hyaluronan of different sizes on human monocytes/macrophages angiogenic behavior in colorectal and breast carcinoma. *In vitro,* treatment of monocytes/macrophages with lysates and conditioned media from a breast, but not from colorectal, carcinoma cell line plus high molecular weight hyaluronan induced: i) an increased expression of angiogenic factors VEGF, IL-8, FGF-2 and MMP-2, ii) increased endothelial cell migration and iii) a differential expression of hyaluronan-binding protein TSG-6. Similar results were observed in monocytes/macrophages

derived from breast cancer patients treated with tumor lysates. Besides, macrophages primed with high molecular weight hyaluronan and inoculated in human breast cancer xenograft tumor increased blood vessel formation and diminished TSG-6 levels. In contrast, the effects triggered by high molecular weight hyaluronan on monocytes/macrophages in breast cancer context were not observed in the context of colorectal carcinoma. Taken together, these results indicate that the effect of high molecular weight hyaluronan as an inductor of the angiogenic behavior of macrophages in breast tumor context is in part consequence of the presence of TSG-6.

Introduction

Hyaluronan (HA), an anionic non-sulfated glycosaminoglycan, is a main component of the extracellular matrix in tissues. HA functions are well known to be size-dependent. At homeostasis, high-molecular weight HA (HMW HA: 1500-1800 kDa) is predominant and has hydrodynamic properties, whereas low-molecular weight HA (LMW HA: 100-300 kDa) is present mainly during inflammation [1]. It is well known that HA binds several cell surface receptors such as CD44, TLR4 and RHAMM and its size can influence the receptor activation and downstream signaling [2]. Even more, tumor necrosis factor (TNF)-stimulated gene 6 (TSG-6) is a hyaluronan binding protein. TSG-6 has a crucial role in the formation of HA crosslinking with other matrix components, such as the serine protease inhibitor inter-α-inhibitor (IαI) heavy chains (HCs) which allows stabilization and structural integrity of the extracellular matrix [3-5].

On the other hand, HA is a crucial player in many processes associated with cancer [6] and has been detected in tissues [6], as well as serum, in multiple types of cancer [7]. Particularly, HA was detected in serum from breast cancer patients [8, 9]. In several tumors, LMW HA promotes spreading by stimulating angiogenesis and creating a microvascular network [10]. However, we have previously demonstrated that in colorectal carcinoma exogenous LMW but not HMW HA, significantly reduced tumor growth *in vitro* and *in vivo*, in part by its immunostimulatory action [11]. Although in breast carcinoma, LMW HA and not HMW HA may contribute to tumor progression [12]. These controversial results might be due to not considering the impact on tumor-associated cells, such as monocytes/macrophages and factors that modulates HA structure and function.

Monocytes (Mo) are circulating innate immune cells. Some monocytes migrate into tissues or to the sites of damage or infection where they subsequently develop into different type of monocyte-derived macrophages (MØ). Cells of this lineage are jointly described to as mononuclear phagocytes or monocytes/macrophages (Mo/MØ) [13]. These cells participate in many states of physiological and pathological processes, in addition to their role in the immune response [14]. MØ are critical modulators of the tumor microenvironment, although its behavior differs considerably among tumors. They are classically known as tumor-associated macrophage (TAM) and considered an M2 type or regulatory MØ, which are able to promote angiogenesis [15]. Mo/MØ are able to bind HA which induces intracellular signals [16, 17], however, the role that different sized HA plays on MØ behavior in the presence of tumor factors is not well known, defining their anti or pro-tumor effect. Moreover, TSG-6 is not in general a constitutively expressed protein in normal adult tissues and during inflammation its expression is upregulated. This HA binding protein is produced by activated MØ modulating inflammation process as a consequence of tissues injury [5, 18, 19]. However, its mechanism of action and its role in Mo/MØ behavior are not fully understood in cancer. Consequently, the aim of our work was to evaluate HA (LMW and HMW) effect on human Mo/MØ angiogenic behavior in two different tumor microenvironments, colorectal and breast. It is well known that tumor necrosis is related to a more angiogenic and inflammatory microenvironment in various types of cancer [20, 21], among them breast cancer [22]. That is why we evaluated Mo/MØ behavior exposed to factors from tumor cell lysates or cell supernatants. On the other hand, we analyzed the role of TSG-6 as a modulator of HA function within these tumor microenvironments.

Results

HA fails to modulate phenotypic markers of Mo/MØ in tumor microenvironments.

To characterize peripheral blood mononuclear cells (PBMCs) derived Mo/MØ by expression of cell surface antigens, we evaluated by flow cytometry different cell surface markers: CD14, HLA, CD80 and CD206. Monocytes were gated by CD14 positive expression and the co-expression of the markers was analyzed to immune characterize Mo/MØ. On average, 81% of the cells in culture expressed this marker, indicating a higher homogeneity of the culture and their monocytic lineage (Fig.1). Besides, no differences were found between treatments. HA (HMW or LMW) and factors from tumor cell lysates (TL) were not able to modulate the expression of these molecules in our experimental conditions (Fig.1A). Similar

results were observed during treatment of macrophages exposed to conditioned media (CM) (Fig. 1B). TL and CM concentration does not affect Mo/MØ viability (Fig. 2). Therefore, HA plus TL or CM were not able to modulate the Mo/MØ surface markers. Since our aim was to study the modulation of HA on Mo/MØ angiogenic function in tumor context, we analyzed the expression of pro-angiogenic molecules: VEGF, FGF-2, IL-8 and MMPs.

HMW HA increased VEGF production in Mo/MØ in breast but not in colorectal carcinoma microenvironment.

As it was previously mentioned, TAMs induce tumor vascularization by releasing several factors, including VEGF which is the main angiogenic factor. Thus, VEGF expression was analyzed to evaluate the effect of HA (LMW and HMW) on Mo/MØ pulsed with TL from breast cancer cell line MDA-MB-231 (MTL) or colorectal carcinoma cell line LoVo (LTL). Mo/MØ treated with MTL plus HMW HA significantly increased VEGF levels (NRQ: 3,769 ± 0,9416) when compared to MTL without HA (NRQ: 0,3000 ± 0,1732) or MTL plus LMW HA (NRQ: 0,3587 ± 0,2071) (Fig. 3 A). No differences were observed between treatments with LTL (Fig. 3 A). In order to evaluate VEGF expression modulated by CM we performed a RT-qPCR. Mo/MØ were treated with CM derived from MDA-MB-231 (MCM) or LoVo (LCM). VEGF levels increased when Mo/MØ were treated with MCM plus HMW HA (NRQ: 3.216 ± 0.06561) in comparison with MCM treatment without HA (NRQ: 0.1100 ± 0.0110) and plus LMW HA (NRQ: 0.0 ± 0.0) (Fig. 3 B). Mo/MØ treated with LCM plus HA (LMW or HMW) showed no differences in VEGF expression levels. Taken together these results indicate that HMW HA is able to increase VEGF levels in Mo/MØ in a breast carcinoma context.

HMW HA increased the expression of IL-8 and FGF-2 in Mo/MØ in breast but not in colorectal carcinoma microenvironment

Mo/MØ express and secrete other important angiogenic factors, like IL-8 and FGF-2. Consequently, we evaluated the mRNA expression levels of IL-8 and FGF-2 of Mo/MØ pulsed with TL or CM with or without HA. In concordance with VEGF synthesis levels, Mo/MØ incubated with MTL plus HMW HA increased IL-8 expression levels (NRQ: 5.761 ± 1.461) when compared to the treatments with MTL without HA (NRQ: 2.630 ± 0.5698) or MTL plus LMW HA (NRQ: 1.756 ± 0.1945) (Fig. 3 C). When we analyzed IL-8 levels from Mo/MØ treated with CM, we observed a significant increase of IL-8 with the treatment with MCM plus HMW HA (NRQ: 10.61 ± 0.4400) (Fig. 3 D). FGF-2 expression levels in Mo/MØ

treated with MTL plus HMW HA (NRQ: 2.972 ± 0.8020) showed an increased tendency when compared to MTL without HA (NRQ: 2.461 ± 0.5345) and a significant increase comparing to BC (NRQ: 0.3447 ± 0.09539) (Fig. 3 E). Similarly, Mo/MØ treated with HMW HA plus MCM increased FGF-2 expression levels (NRQ: 4.150 ± 0.2656) comparing to MCM (NRQ: 2.280 ± 0.3600) and MCM plus LMW HA (NRQ: 0.9050 ± 0.3650) (Fig. 3 F). Mo/MØ treated with LTL or LCM plus HA (LMW or HMW) showed no differences in the mRNA expression levels of IL-8 and FGF-2 (Fig. 3 C-F).

HMW HA treatment modulated MMPs expression levels and activity in Mo/MØ in a breast but not in colorectal carcinoma microenvironment

In tumor context, Mo/MØ upregulate MMP-2 and MMP-9 production and their proteolytic activity triggers the degradation of the extracellular matrix and the bioavailability of angiogenic factors [23]. Thus, we analyzed MMPs activity by gelatin zymography as another angiogenic mechanism regulated by HA. MMP-9 activity showed no difference between HA treatments with TL and CM (Fig. 4 A and E) in Mo/MØ. However, the treatment with MTL plus HMW HA increased MMP-2 activity (NRQ: 5.685 ± 0.2162) in these cells (Fig. 4 C) compared to BC. The HA action was not only restricted to HMW HA, the treatment with MTL plus LMW HA also increased its activity (NRQ: 6.278 ± 0.5816) (Fig. 4 C). MMP-2 showed similar activity in Mo/MØ PBMCs pulsed with LTL both treatments and controls (Fig. 4 C). In addition, to corroborate these results we analyzed mRNA levels of MMP-9 and MMP-2. As expected, MMP-9 expression levels showed no differences during the treatments (Fig. 4 B). MMP-2 mRNA levels significantly increased with MTL plus HMW HA treatment (NRQ: 5.685 ± 0.2162) with respect to MTL (NRQ: 3.343 ± 1.220) (Fig. 4 D). MCM or LCM treatments of Mo/MØ did not modulate MMPs activity or their expression levels (Fig. 4 F and H).

Higher in vitro migration of ECs towards Mo/MØ supernatants when treated with HMW HA in a breast but not in colorectal carcinoma microenvironment

We decided to test the migration of ECs *in vitro*, as a way of evaluating the functional modulation of these cells involved in the vessel formation. As expected, significantly higher migration of ECs was observed towards the supernatants of Mo/MØ treated with MTL plus HMW HA (index cell migration: 6.830 ± 1.465) when compared to MTL without HA (index cell migration: 3.523 ± 0.5100) and MTL plus LMW HA (index cell migration: 1.380 ± 0.2287) (Fig. 5). However, the treatments of Mo/MØ with LCM showed no differences in the

migration levels of ECs (Fig. 5). Moreover, differential migration was observed in ECs towards Mo/MØ supernatants derived in the presence of MTL (index cell migration: 3.523 ± 0.5100) when compared with LTL (index cell migration: 0.7459 ± 0.1051). We were not able to perform this experiment with tumor cells CM since MCM as well as LCM are chemoattractants of ECs *per se* and did not allow us to evaluate differences among the treatments.

Mo/MØ treated with HMW HA modulated HA receptors expression levels in a breast carcinoma microenvironment

HA induces cell signaling through several receptors such as CD44, TLR-4 and RHAMM. Since these receptors are involved in HA responses in Mo/MØ cells, we examined the effect of TL or CM with or without HA addition on their mRNA expression levels. The treatment with HWM HA induces an increase of CD44 expression levels (NRQ: 1.676 ± 0.3466) with respect to BC (NRQ: 1.107 ± 0.1700), but has no significant effect on TLR-4 or RHAMM expression levels (Fig. 6 A, C and E). Besides, MTL plus HMW HA significant decreased expression levels CD44 (NRQ: 0.5866 ± 0.02388) and TLR4 (NRQ: 0.4602 ± 0.1234), in comparison to the treatment of MTL without HA (NRQ: 2.043 ± 0.4256), without modulating RHAMM expression levels (Fig. 6 A, C and E). In contrast, no differences were observed among the LTL treatments (Fig. 6 A, C and E). We also evaluated the behavior of Mo/MØ cells exposed to CM from tumor living cells. These CM did not affect CD44, TLR-4 and RHAMM expression levels (Fig. 6 B, D, F). However, MCM plus HMW HA significantly decreased TLR-4 expression levels (NRQ: 0.7250 ± 0.01500) in comparison to MCM without HA treatment (NRQ: 1.635 ± 0.03500) (Fig. 6 D). CD44 and RHAMM levels showed no difference between MCM treatments (Fig. 6 F). As for LCM treatments, no differences were observed among them in the expression levels of the receptors analyzed (Fig. 6 B, D and F).

Mo/MØ preincubated with HMW HA increased the tumor vasculature in the breast cancer model

We tested whether the in vitro angiogenic effects could be observed in an in vivo model. For this purpose, nude mice were injected with MDA-MB-231 or Lovo cells and nine days later animals with similar tumor volume were inoculated with Mo/MØ preincubated with HMW or LMW HA. Tumor volume was measured weekly and we found no differences in tumor growth between treatments (data not shown). Tumors were fixed and sections were stained

with: i) H&E to rule out changes in tumor histology or ii) GSL-1 to analyze ECs forming blood vessel.

We observed that Mo/MØ preincubated with HMW induced a significant increment of the tumor vasculature in the MDA-MB-231 model detected by immunofluorescence intensity (AU) of GSL-1-FITC (AU: 1.759 ± 0.1173) compare to Mo/MØ without treatment (AU: 1.158 ± 0.1193) and pulsed with LMW HA (AU: 1.017 ± 0.07250) (Fig. 7 A). Besides, the tumor vasculature decreased in those animals inoculated with Mo/MØ previously treated with LMW HA in comparison with tumor control (AU: 1.602 ± 0.1307) (Fig. 7 A). However, in LoVo model, we observed no difference in the vasculature after all treatments (Fig. 7 B). Tissues section for each model and treatments presented similar tumor structure without necrosis areas. In conclusion, in vivo data confirm and is in concordance with the *in vitro* results.

TSG-6 production by Mo/MØ is deregulated with HMW HA in a breast carcinoma microenvironment

Taking into account the results presented above we could indicate that there is a factor whose expression in Mo/MØ is triggered by HMW HA in breast carcinoma context but not in colorectal. Therefore we decided to evaluate gene and protein expression levels of TSG-6, a hyaluronan-binding protein that modulates its structure and function in inflammatory or tissue injury process [5, 24]. Firstly, GEO2R was applied to screen TSG-6 expressed mRNAs levels in macrophages. TSG-6 was screened in two mice datasets: breast (GSE18404) and in colorectal (GSE67953) carcinoma; TSG-6 was expressed in both datasets but no differences were found between TAMs and spleen macrophages (Fig. 8). We observed that TSG-6 mRNA expression levels were not modulated significantly in Mo/MØ treated with LMW or HMW HA. However, we found different TSG-6 expression levels when Mo/MØ were pulsed with MTL (NRQ: 5.860 ± 2.711) compared to BC (NRQ: 0.3615 ± 0.1206) and LTL (NRQ: 1.233 ± 0.4856) (Fig. 9 A). Besides, TSG-6 mRNA levels decreased in Mo/MØ treated with MTL plus HMW HA (NRQ: 0.4540 ± 0.1535) in comparison to MTL without HA (NRQ: NRQ: 5.860 ± 2.711). Whereas, Mo/MØ pulsed with LTL, with or without HA, showed no differences in TSG-6 mRNA levels (Fig. 9 A). In the case of CM treatments, MCM plus HMW HA significantly increased TSG-6 mRNA levels (NRQ: 18.35 ± 4.835) when compared to MCM treatment without HA (NRQ: 3.703 ± 1.603) (Fig. 9 C).

In addition, we analyzed TSG-6 protein expression through Western blot in Mo/MØ supernatants and we detected two species: i) ~35 kDa corresponding to free TSG-6 and ii) ~120 kDa corresponding to the complex generated by the heavy chain (HC) of IαI and TSG-6, as have been documented by other authors [25]. We found that in Mo/MØ supernatants free TSG-6 was increased with MTL treatment (AU: 24.73 ± 3.472) or LTL treatment (AU: 19.78 ± 2.301) with respect to BC (AU: 2.773 ± 1.337) (Fig. 9 B). MTL plus HMW HA diminished the 120 kDa species, when compared to MTL (AU: 10.69 ± 1.297). LTL plus HMW HA (10.69 ± 1.297 AU) diminished the 120 kDa species, when compared LTL (11.56 ± 1.054 AU) without HA treatment (Fig. 9 B).

We also performed TSG-6 western blot from Mo/MØ supernatants treated with MCM or LCM (Fig. 9 D). MCM plus HMW HA increased ~35 kDa species corresponding to free TSG-6 (AU: 9.755 ± 0.07500) with respect to MCM (AU: 4.675 ± 0.3850) and BC (AU: 2.773 ± 1.337) (Fig. 9 D). However, the ~120 kDa species, corresponding to TSG-6·HC, significantly decreased with MCM plus HMW HA (AU: 5.347 ± 1.509) when compared to MCM without HA (AU: 10.78 ± 2.289). This species corresponding TSG-6·HC were not detected in the supernatants of Mo/MØ treated with LCM with or without HA (Fig. 9 D right panel).

Mo/MØ preincubated with HMW HA decreased TSG-6 levels in breast cancer model

In order to evaluate the intrinsic effects of these molecules in the tumor stroma, tumor sections of xenograft models were stained with TSG-6 and HA by immunofluorescence. In the MDA-MB-231 model, mice inoculated with Mo/MØ without treatment (AU: 3.201 ± 0.3712) increased TSG-6 levels respect to control mice (without inoculation of Mo/MØ) (AU: 1.624 ± 0.1989) (Fig. 10 A). Besides, mice inoculated with Mo/MØ preincubated with HMW HA, which presented a significant increment of the tumor vasculature, decreased TSG-6 immunofluorescence intensity (AU: 1.820 ± 0.4308) when compared to mice inoculated with Mo/MØ without treatment (AU: 3.201 ± 0.3712) (Fig. 10 A). In contrast, TSG-6 levels in the LoVo model presented no differences among treatments (Fig. 10 B). These TSG-6 results from the *in vivo* model are in concordance with the *in vitro* results obtained for TSG-6 mRNA levels (Fig. 9 A). When we analyzed total endogenous HA levels, we found no significant differences in the MDA-MB-231 model. Contrary, tumor sections derived from mice of the LoVo model inoculated with Mo/MØ preincubated with HMW HA, presented a

significant increment in total HA (Fig. 10 B). Thus, despite similar or dissimilar accumulation of HA in the tumor is the differential expression of TSG-6 that might affect HA action in Mo/MØ within both tumor models, which also affect their angiogenic behavior.

TSG-6 levels were deregulated when Mo/MØ derived from cancer patients were treated with HMW HA and tumor tissues lysates

To further evaluate HA effect on human Mo/MØ angiogenic behavior we used Mo/MØ derived from cancer patients (breast and colorectal) and we prepared from each patient lysates from tumor tissue (TTL) and from normal tissue adjacent to the tumor (NATL). In Mo/MØ samples derived from breast cancer patients (ER-positive), free TSG-6 protein levels (~35 kDa species) increased with TTL treatment plus HMW HA (AU: 19.94 ± 0.7000) respect to TTL without HA (AU: 7.485 ± 2.045) (Fig. 11 A, right panel). Free TSG-6 levels did not show significant differences among NATL treatments (Fig. 11 B, right panel). As for, TSG-6·HC (~120 kDa species) it showed a decrease when Mo/MØ were treated with breast TTL plus HMW HA (AU: 6.215 ± 1.225) in comparison to TTL (AU: 16.34 ± 2.095) (Fig. 11 A, left panel), but among NATL treatments we did not observe significant differences (Fig. 11 B, left panel). Mo/MØ samples derived from colorectal carcinoma showed no significant differences between TTL or NATL treatments.

Discussion

Macrophages derived from monocytes, exhibit a diversity cell behavior, beyond its immunological role. These cells secrete crucial factors for growth and remodeling of the microvasculature during angiogenesis. Despite vast investigations of Mo/MØ response to tumor cells and inductors of angiogenesis, few studies are focused on evaluating their behavior considering the extracellular matrix interaction. This issue is an important point of study to develop novel cancer therapies that target angiogenesis and simultaneously immunosuppression. For example, it has been demonstrated that disruption of angiogenesis substantially enhances the efficacy of immune-based cancer therapies [26].

As it was previously mentioned, HA is one of the extracellular matrix components that can modify the behavior of both tumor and immune cells types [1]. HA interacts with Mo/MØ inducing their migration, the release of chemokines, cytokines, growth factors and expression of MMPs [27]. However, it has been observed that HA released by tumor cells selectively deactivate Mo/MØ inhibiting their antitumor immune response [28, 29]. Recent works

showed that HA derived from breast cancer induces MØ to acquire an immunosuppressive or M2-like phenotype [30]. It is well established that HA size is critical for its function. Thus, we used LMW HA and HMW HA of defined size in our experiments. We observed that HA, both as LMW or HMW, in the presence of tumor factors, either from tumor lysates or conditioned media from breast (MTL) or colorectal (LTL) cells, did not affect surface markers that define the MØ phenotype [31]. Besides, it is important to consider that Mo/MØ behavior and function is not only defined by cell surface markers, and a better characterization may also be possible *in vivo* based on the paracrine factors that they secrete.

To evaluate Mo/MØ as an inductor of angiogenesis under HA treatments in a tumor context, we analyzed the expression of biosynthesis of VEGF, the main angiogenic factors (Fig. 3 A and B). We evaluated Mo/MØ behavior between the different tumor types and exposing them to tumor cells lysates (TL) or soluble factors from tumor cells conditioned media cells (CM). These cells need to be stimulated to produce VEGF and HA by itself was not able to induce this expression. Even more, HMW HA but only in the presence of breast carcinoma antigens (MTL or MCM) increased significantly VEGF mRNA levels (Fig. 3 A and B). Similar results were observed when we evaluated other pro-angiogenic molecules like IL-8 and FGF-2 (Fig. 1 C-F)[32]. Thus, it is possible to hypostatize that there are different factors in the tumor lysates or conditioned media from breast cancer cells, but not in colorectal cancer cells, that could be modulating the function of HWM HA on Mo/MØ. Besides, we found a significant increase in MMP-2 gelatinolytic activity when Mo/MØ were treated with HA (LMW or HMW) in the presence of MTL (Fig. 4 C). Although mRNA MMP-2 levels increased only during the treatment with MTL plus HMW HA (Fig. 4 D). It was documented that MMP-2 cleaves collagen type IV and it is associated with ECs migration, affecting their capacity to generate new vessel [33]. Besides, it was previously demonstrated that HA-CD44 interaction allows the activation of MMP-2 [34]. Thus, factors that modulate HA function might be directly connected with the MMP-2 activity, since we observed a modulation with MTL but not with LTL treatment. To further study the biological function of angiogenic factors released with the different treatments, we analyzed the migration capability of ECs towards the Mo/MØ supernatants. A higher migration was observed with MTL and even more with MTL plus HMW HA treatment (Fig. 5), suggesting that factors in MTL induce an HA with pro-angiogenic action on Mo/MØ. In turn these cells release VEGF, IL-8, FGF-2 and MMP-2 that stimulate ECs migration. Similar results were observed when we evaluated angiogenesis *in vivo* analyzing the vessels by detection of ECs. We found a significant increase of ECs

staining in tumor tissue of MDA-MB-231-bearing mice that were treated with MØ primed with HMW HA but no differences were detected in LoVo-bearing mice (Fig. 7).

To study HA receptors that are involved in the Mo/MØ responses, we evaluated CD44, TLR-4 and RHAMM mRNA expression levels (Fig. 6). It has been shown that CD44 and TLR-4 are involved in immune deactivation of human Mo/MØ cells [23] Actually, modulation of this receptors expression affects their immune phenotype and function within tumor microenvironment [1]. We only observed modulation of these receptors in Mo/MØ exposed to treatments with antigens from breast cancer cells lines. We observed that HMW HA treatment induced a significant downregulation of CD44 and TLR-4 expression in Mo/MØ in the presence of MTL, for TLR-4 we also observed a significant decrease with MCM plus HMW HA. Thus, the decrease of HA receptors expression could be associated with angiogenesis and involved in HA response *in vivo* according to the type of tumor microenvironment. In light of these results, we carried out subsequent experiments to identify the factor/factors that is/are modulating the HA function and in turn Mo/MØ angiogenic behavior in both types of cancer. Although HA is not covalently linked to a core protein, it can interact with HA-binding proteins or hyaladherins, that in turn modulate HA structure and function. TSG-6, is a well-characterized hyaladherin, with an HA-biding site located within a domain called "link module" [18, 24]. For example, it has been observed that aggregation of HA IαI-induced is dependent on TSG-6 and allows the stabilization of the extracellular matrix [24]. Thus, alteration of TSG-6 might affect HA function. We suggest that the differences found in Mo/MØ behavior when they were exposed to different sizes of HA and different tumor types could be associated with HA-binding proteins that in turn modulate HA action. In most cell types, the expression of TSG-6, as immunoregulator mediator, is stimulated by cytokines or factors released during inflammation, inflammation-like or injury processes. It is proposed that TSG-6 controls inflammation response and maintains the extracellular matrix homeostasis [18].

For the first time, we detected a reduction in the expression levels of the bands corresponding to the complex TSG-6·HC only when Mo/MØ were treated with HA (HMW or LMW) plus MTL, LTL or MCM. Markedly, TSG-6·HC protein expression was only modulated in breast tumor context. Indicating that specific tumor factors could induce an immunosuppressive and angiogenic action of TAMs by modulating TSG-6, and its expression within the tumor is also modulated by the interaction with extracellular matrix components such as HA. The TSG-

6·HC complex is indicative of the enzymatic activity of TSG-6. It is well known that TSG-6 catalyze the transfer of the IαI HC to HA, affecting the activity of this proteinase inhibitor [3, 4] as well as HA structure, the binding capacity to its receptors and therefore its function [24].

Even more, we used xenograft nude mice models, which does not allow the development of adaptive immune response, but innate immune response is still intact and offers a tumor milieu to study Mo/MØ function and regulation of angiogenesis. We observed that the treatment of Mo/MØ induced an increase of TSG-6 that was significantly reduced during the treatment of Mo/MØ preincubated with LMW HA in breast carcinoma model (Fig. 10 A). These results are in concordance of in vitro results where TSG-6 mRNA levels decreased in Mo/MØ treated with MTL plus HMW HA in comparison to MTL without HA. When HA expression was analyzed in tumor tissues, no changes were detected in the breast carcinoma model. This indicates that different function of HA is dependent on factors or antigens of the tumor microenvironments than the amount of HA present within the tissues. The analysis of Mo/MØ treated with tumor or normal adjacent tissue derived from patients with invasive breast carcinoma (ER+, stage I or II) or colorectal carcinoma (stage I or II) allowed us to extend our results in the context of different types and stages of breast and colorectal carcinoma. Mo/MØ cells treated with TTL from breast cancer patients plus HMW HA also modulates both species of TSG-6 (HC bonded and free). Besides, no modulations were observed from colorectal cancer and normal tissues. Considering our results, we can conclude that modulation of TSG-6 activity and expression is differentially modulated according to tumor type. However, further studies will be necessary to find the factors present in breast carcinoma that are involved in this HA-TSG-6 regulation loop.

As for Mo/MØ treated with colorectal carcinoma antigens, HMW HA did not affect HA receptors, TSG-6 nor their angiogenic behavior. Interestingly, the role of macrophages in colorectal carcinoma is controversial. Some studies support that TAMs exhibit tumor-suppressive abilities, whereas others report that these cells contribute to colorectal cancer promotion [35]. However, it was shown that high density of tumor-associated MØ correlates with poor prognosis in breast carcinoma since this cells were capable of inducing angiogenesis, remodeling the tumor extracellular matrix to aid invasion, modeling breast cancer cells to evade host immune system and recruiting immunosuppressive leukocytes to the tumor microenvironment[36].

Finally, this study showed for the first time that HMW HA, a highly conserved and poorly immunogenic molecule, downregulates TSG-6 levels in Mo/MØ modulating their angiogenic behavior in breast carcinoma milieu, but not in colorectal carcinoma. Even more, CM induced downregulation of TSG-6-HC complex could be essential for in vivo angiogenesis because this effect was not observed in LCM. These findings are of great interest, since it may provide novel breast cancer targets, especially to increase the success of anti-angiogenic agents.

Materials and Methods

Reagents

Pharmaceutical endotoxin-free HA recombinant of definite size: HMW 1.5–1.8 x 106 Da and LMW 1–3 x 105 Da from CPN spol.s.r.o was kindly supplied by Farmatrade.

Cell lines and human blood

LoVo (human colorectal adenocarcinoma) provided by Dr. Lucia Policastro (Instituto de Nanociencia y Nanotecnología, BA, Argentina) and MDA-MB-231 (breast adenocarcinoma) by Roxana Schillaci (IBYME, CABA, Argentina) were maintained with DMEM/F12 supplemented with 10% FBS, 2 mM L-glutamine, 100 U/ml streptomycin and 100 mg/ml penicillin and incubated at 37°C in a 5% CO_2 humidified atmosphere. HMEC-1 (dermal microvascular endothelium) cell line was cultured with DMEM supplemented with 10% FBS, 2 mM L-glutamine, 100 U/ml streptomycin and 100 mg/ml penicillin and incubated at 37°C in a 5% CO_2 humidified atmosphere. In all cell cultures, periodic checkups of cell morphology were performed, as well as strict control of cell line passages (5 -10th passage) and cell line growth rate. In addition, all cell lines were analyzed to discard the presence of mycoplasma contamination by PCR assay.

Peripheral blood samples for human monocyte isolation were obtained from voluntary blood donors and from cancer patients. Tumor tissue as well as normal tissue adjacent to the tumor (NAT) were obtained from cancer patients. Approval was obtained from the Institutional Assessment Committee (CIE) – IRB within the Austral University Hospital (CIE N° 17-006). Informed consent was obtained from participants in accordance with the Declaration of Helsinki.

Tumor lysates and conditioned media

Confluent cultures of LoVo or MDA-MB-231 cells were detached with cold PBS, washed twice in PBS and resuspended in PBS. Cell suspensions ($1{,}2x10^6$ cells/ml) and conditioned media (CM) were frozen at -80°C. The cell suspensions were disrupted by 5 freeze-thaw cycles. To remove large debris, tumor lysates (TL) MDA-MB-231 (MTL) or LoVo (LTL) were centrifuged at 300 rpm for 10 min. The supernatant was collected and passed through a 0.22 mm filter unit. Conditioned media (CM) were collected from supernatants from tumor cell lines MDA-MB-231 (MCM) or LoVo (LCM) cultured ($1{,}2x10^6$ cells) for 6 h without serum. The protein concentration was determined by Bradford assay. As for cancer patient's lysates were prepared using the same protocol for tumor lysates previous mechanical disintegration of the tissues. Lysates derived from tumor tissue (TTL) and from normal tissue adjacent to the tumor (TNAT). The resulting TL or CM were aliquoted and stored at -80°C until use.

Isolation of PBMC-derived Mo/MØ

PBMCs were isolated by the Ficoll-Paque Plus (GE Healthcare) gradient. Cells were plated into 12-well plates for 2 h, removing the non-adherent cells. Then, adhered cells were subsequently cultured overnight in complete RPMI 1640 medium [37]. 24 h later, the medium of the adherent MØ was replaced with RPMI 1640 (FBS free) and were pulsed with either with conditioned media or TL (200 µg/10^6 cells/ml) with or without LMW HA (20 µg/ml) or HMW HA (20 µg/ml). After 24 h cells were centrifuged, characterized by flow cytometry and used for experiments.

MTS

Cell viability assay was measured by MTS method (ab197010, Abcam) as described in the manufacture protocol. Mo/MØ treated with MTL or LTL (0, 100, 200 and 400 µg/ml) were seeded in 96-well plates at a density of 6×10^3 per well and 3 hours before the treatments ended the MTS dye was added, and then incubated for 3 hours in the dark. The optical density (OD) values were measured at 490 nm.

Flow cytometry analyses

Staining and flow cytometric analyses of PBMCs derived MØ were carried out using standard procedures. Briefly, 10^6 cells were blocked with PBS-1% BSA for 45' and then were stained on ice for 30 min with different conjugated antibodies: anti-CD14; anti-MHC-II (G46-6); anti-CD80 (L307.4); and anti-CD206 (all from BD Biosciences). Cells were washed thoroughly with PBS-1% BSA and subjected to flow cytometry (FACS CANTO II-BD). Data were analyzed using Flow 7.6.2 software.

ELISA assays

VEGF expression levels were determined by a sandwich ELISA assay (DY293B, R&D Systems™) from free-cell conditioned media. The assays were carried out according to the instructions provided by the manufacturer.

RT-qPCR

Total RNA was extracted by Tri Reagent (TR 118, Molecular research center, Inc.). RNA quantification was evaluted by spectrophotometry. Then, 2 µg of RNA was reverse transcribed with 200U RT M-MLV Reverse Transcriptase (M1701, Promega) and 2,5 pmol/µl of Oligo (dT) primers (GenBiotech). cDNAs were then subjected to real time quantitative PCR (RT-qPCR) using FastStart SYBR Green Master (04673484001, Roche) and 200 nM of each specific primer (Invitrogen, life technologies™):

IL-8: forward 5'-AAGGAAAACTGGGTGCAGAG-3' and reverse 5'-GGCATCTTCACTGATTCTTGG-3'

FGF-2: forward 5'-CCTGGCTATGAAGGAAGATGG-3' and reverse 5'-TCGTTTCAGTGCCACATACC-3'

TSG-6: forward 5'-CATATGGCTTGAACGAGCAGC-3' and reverse 5'-CTTTGCGTGTGGGTTGTAGC-3'

RHAMM: forward 5'- TGGAAAAGATGGAAGCAAGG-3' and reverse 5'-CCAGTGTAGCATTATTTGCAGAG-3'

CD44: forward 5'-GTGATGGCACCCGCTATG-3' and reverse 5'-ACTGTCTTCGTCTGGGATGG-3'

TLR4: forward 5'- TGAGCAGTCGTGCTGGTATC-3' and reverse 5'-CAGGGCTTTTCTTGAGTCGTC-3'

GAPDH: forward 5'-GGGGCTGCCCAGAACATCAT-3' and reverse 5'-GCCTGCTTCACCACCTTCTTG-3'

PCR conditions were: 90 seconds at 94°C and then 40 cycles of 30 seconds at 94°C, 30 seconds at 60°C and 30 seconds at 72°C. Values were normalized to levels of GAPDH housekeeping gene.

Western blot

To analyze TSG-6 biosynthesis in MØ supernatants, equal amounts of protein were resolved by 0.1% SDS-10% polyacrylamide gel denaturing electrophoresis (SDS-PAGE) and transferred to a nitrocellulose membrane. The membranes were incubated overnight at 4°C with RAH-1 a polyclonal human TSG-6 antibody[38] (kindly supplied by Dr. Anthony Day) and then incubated for 1 hour at RT with horseradish peroxidase-labeled secondary antibody. Finally, HRP chemiluminescence reaction was detected using a stable peroxide solution and an enhanced luminol solution. Images were obtained with ImageQuant 4000 mini bioluminescent image analyzer (GE HealthCare LifeSciences) and analyzed using ImageJ.

Gelatin zymography

Matrix Metalloproteinases (MMPs) activity in MØ supernatants was determined by gelatin zymography [39] . Conditioned media was run on a 10% SDS PAGE containing 0.1% gelatin (Sigma-Aldrich). Following electrophoresis, gels were washed with 50 mM Tris-ClH pH 7.5, 2.5% Triton X-100 30 min, 50 mM Tris-ClH pH 7.5, 2.5% Triton X-100, 5 mM $CaCl_2$, 1 mM $ZnCl_2$ 30 min and 50 mM Tris-ClH pH 7.5, 2.5% Triton X-100, 10 mM $CaCl_2$, 200 mM NaCl 48 h at 37°C. The gel was stained with Coomassie Brilliant Blue R-250 for 30 min at room temperature. Gelatinase activity was visualized by negative staining; gel images were obtained with a biomolecular imager (ImageQuant LAS 4000 mini) and were subjected to densitometric analysis using ImageJ 1.50b software package (National Institutes of Health). Fold change MMP-2 and MMP-9 activity was obtained by normalizing values to untreated samples.

In vitro endothelial cell migration assay

In vitro migration was performed using a 48-Transwell microchemotaxis Boyden Chamber unit (Neuroprobe, Inc.). HMEC-1 ($1.5x10^3$ cells/well) were placed in the upper chamber and conditioned medium of the treatments were applied to the lower chamber of the transwell

unit. As a negative control cells were exposed to DMEM and RPMI without FBS and as a positive control a medium rich in angiogenic factors was used. The chamber was left for 4 hours at 37°C in a 5% CO_2 humidified atmosphere. Cells attached to the lower side of the membrane were fixed in 2% formaldehyde and stained with 4′,6-diamidino-2-phenylindole dihydrochloride (DAPI, Sigma-Aldrich). Images from 3 representative visual fields were captured using Nikon Eclipse E800 fluorescence microscope and were analyzed using CellProfiler software (www.cellprofiler.com), and the mean number of cells/field ± SEM was calculated.

Tumor xenograft model

Six-to-eight-week-old male nu/nu mice were purchased from Comisión Nacional de Energía Atómica, Ezeiza, Buenos Aires, Argentina. Animals were maintained at our Animal Resources Facilities (CIBA, CIT NOBA) in accordance with the experimental ethical committee and with the NIH Guide for the Care and Use of Laboratory Animals (eighth edition). MDA-MB-231 or LoVo cell suspension ($1x10^7$ cells/0.1 ml) was injected subcutaneously in the dorsal flank of mice. After 9 days, PBMCs derived Mo/MØ treated or not with LMW or HMW HA were inoculated subcutaneously near the base of the tumor. On day 29 mice were sacrificed and tumors were removed, fixed in 10% formalin and embedded in paraffin. Before staining, 3-µm sections were deparaffinized and dehydrated.

Detection of angiogenesis in tumor tissues

Slides were rinsed with PBS and dye with DAPI 0.3 µg/ml plus fluorescein labeled Griffonia (Bandeiraea) Simplicifolia Lectin I 20 µg/ml (GSL I; FL-1101, Vector Laboratories) that binds specifically to endothelial cells in mouse tissues [40]. The sections were rinsed with PBS and then mounted on microscope slides. Images of the stained sections were taken with a Nikon Eclipse E800 fluorescence microscope. Microvessels were quantified with ImageJ.

Immunostaining of TSG-6 and HA in tumor tissues

Slides were rinsed with PBS and incubated overnight at 4°C with rabbit anti-human polyclonal against TSG-6 (RAH-1)[38] and HA binding protein (385911, Calbiochem). Afterward, the tissue slices were washed three times in PBS and then incubated for 1 h at 4°C with secondary rabbit antibody conjugated with Texas Red® (TI-1000, Vector Laboratories) and streptavidin conjugated with FITC (31274243, Immunotools). The sections were rinsed

with PBS, dye with DAPI 0.3 µg/ml and then mounted on microscope slides. Images of the stained sections were taken with a Nikon Eclipse E800 fluorescence microscope and quantified with ImageJ.

Microarray datasets processing

Publicly available mice microarray datasets GSE18404 (breast carcinoma) and GSE67953 (colorectal carcinoma) were used for comparing differential TSG-6 expression levels in TAMs and spleen MO. In each dataset, NCBI GEO2R tool (http://www.ncbi.nlm.nih.gov/geo/geo2r/), was used to analyze TSG-6 mRNA expression levels.

Statistical analysis

For statistical analysis, 95% confidence intervals (CI) were determined by calculating arithmetic mean values and variance (standard deviation, SD) of three independent experiments. To evaluate whether differences between the values obtained were significant, analysis of variance (ANOVA, Tukey Test) was used to evaluate the differences between values of more than two experimental groups. The software Prism (GraphPad, San Diego, CA, USA) was used, considering a p value<0.05 as statistically significant.

Acknowledgments

We thank Natalia Menite for technical assistance in flow cytometry and Gaston Villafañe for laboratory animal assistance from Centro de Investigaciones Báscias y Aplicadas (UNNOBA); biochemist Lucia Romano, as support staff for research and development from CIT NOBA, for technical assistance in immunohistochemistry analysis; Daniel Petraglia for technical assistance in histopathological analyzes; the surgery service of the Clínica Centro; the gynecology (C. Lopez, MD and L. Walker, MD), pathology and surgery service and the clinical analysis laboratory from Hospital Interzonal General de Agudos Dr. Abraham F. Piñeyro; and Dr. Anthony Day for providing the TSG-6 primers sequences, RAH-1 antibody and protocols for western blot and immunofluorescence.

Author contributions

FS, DV, AI, IS, IC and AB performed experiments. PG and VG contributed with essential human samples. FS and LA planned experiments, analyzed data and wrote the manuscript. MG and AP revised the paper. IS contributed with essential paper revision. LA conceived and designed the research. All authors gave their final approval for publication.

Funding details

This work was supported by Universidad Nacional del Noroeste de la Pcia de Bs. As. (UNNOBA); UNNOBA-CONICET under Grant PIO 2015-15720150100010CO; Instituto Nacional del Cancer, Ministerio de Salud under Grant ID31/2015; EU Horizon 2020 project RISE-2014 under Grant 645756; Subsidios de investigation bianuales, UNNOBA under Grant 01117/2017; and Fundación Alberto J. Roemmers 2018.

References

1. Spinelli, F. M., Vitale, D. L., Demarchi, G., Cristina, C. & Alaniz, L. (2015) The immunological effect of hyaluronan in tumor angiogenesis, *Clinical & translational immunology.* **4**, e52.
2. Cyphert, J. M., Trempus, C. S. & Garantziotis, S. (2015) Size Matters: Molecular Weight Specificity of Hyaluronan Effects in Cell Biology, *International journal of cell biology.* **2015**, 563818.
3. Rugg, M. S., Willis, A. C., Mukhopadhyay, D., Hascall, V. C., Fries, E., Fulop, C., Milner, C. M. & Day, A. J. (2005) Characterization of complexes formed between TSG-6 and inter-alpha-inhibitor that act as intermediates in the covalent transfer of heavy chains onto hyaluronan, *The Journal of biological chemistry.* **280**, 25674-86.
4. Briggs, D. C., Birchenough, H. L., Ali, T., Rugg, M. S., Waltho, J. P., Ievoli, E., Jowitt, T. A., Enghild, J. J., Richter, R. P., Salustri, A., Milner, C. M. & Day, A. J. (2015) Metal Ion-dependent Heavy Chain Transfer Activity of TSG-6 Mediates Assembly of the Cumulus-Oocyte Matrix, *The Journal of biological chemistry.* **290**, 28708-23.
5. Day, A. J. & Milner, C. M. (2018) TSG-6: A multifunctional protein with anti-inflammatory and tissue-protective properties, *Matrix biology : journal of the International Society for Matrix Biology.*
6. Tammi, R. H., Kultti, A., Kosma, V. M., Pirinen, R., Auvinen, P. & Tammi, M. I. (2008) Hyaluronan in human tumors: pathobiological and prognostic messages from cell-associated and stromal hyaluronan, *Seminars in cancer biology.* **18**, 288-95.
7. Cowman, M. K., Lee, H. G., Schwertfeger, K. L., McCarthy, J. B. & Turley, E. A. (2015) The Content and Size of Hyaluronan in Biological Fluids and Tissues, *Frontiers in immunology.* **6**, 261.
8. Delpech, B., Chevallier, B., Reinhardt, N., Julien, J. P., Duval, C., Maingonnat, C., Bastit, P. & Asselain, B. (1990) Serum hyaluronan (hyaluronic acid) in breast cancer patients, *International journal of cancer.* **46**, 388-90.

9. Yahya, R. S., El-Bindary, A. A., El-Mezayen, H. A., Abdelmasseh, H. M. & Eissa, M. A. (2014) Biochemical evaluation of hyaluronic acid in breast cancer, *Clinical laboratory.* **60**, 1115-21.
10. Singleton, P. A. (2014) Hyaluronan regulation of endothelial barrier function in cancer, *Advances in cancer research.* **123**, 191-209.
11. Alaniz, L., Garcia, M., Rizzo, M., Piccioni, F. & Mazzolini, G. (2009) Altered hyaluronan biosynthesis and cancer progression: an immunological perspective, *Mini reviews in medicinal chemistry.* **9**, 1538-46.
12. Bourguignon, L. Y., Wong, G., Earle, C. A. & Xia, W. (2011) Interaction of low molecular weight hyaluronan with CD44 and toll-like receptors promotes the actin filament-associated protein 110-actin binding and MyD88-NFkappaB signaling leading to proinflammatory cytokine/chemokine production and breast tumor invasion, *Cytoskeleton.* **68**, 671-93.
13. Ginhoux, F. & Jung, S. (2014) Monocytes and macrophages: developmental pathways and tissue homeostasis, *Nature reviews Immunology.* **14**, 392-404.
14. Murdoch, C. & Lewis, C. E. (2005) Macrophage migration and gene expression in response to tumor hypoxia, *International journal of cancer.* **117**, 701-8.
15. Mantovani, A., Marchesi, F., Malesci, A., Laghi, L. & Allavena, P. (2017) Tumour-associated macrophages as treatment targets in oncology, *Nature reviews Clinical oncology.* **14**, 399-416.
16. Sokolowska, M., Chen, L. Y., Eberlein, M., Martinez-Anton, A., Liu, Y., Alsaaty, S., Qi, H. Y., Logun, C., Horton, M. & Shelhamer, J. H. (2014) Low molecular weight hyaluronan activates cytosolic phospholipase A2alpha and eicosanoid production in monocytes and macrophages, *The Journal of biological chemistry.* **289**, 4470-88.
17. Rayahin, J. E., Buhrman, J. S., Zhang, Y., Koh, T. J. & Gemeinhart, R. A. (2015) High and low molecular weight hyaluronic acid differentially influence macrophage activation, *ACS biomaterials science & engineering.* **1**, 481-493.
18. Milner, C. M. & Day, A. J. (2003) TSG-6: a multifunctional protein associated with inflammation, *Journal of cell science.* **116**, 1863-73.
19. Mittal, M., Tiruppathi, C., Nepal, S., Zhao, Y. Y., Grzych, D., Soni, D., Prockop, D. J. & Malik, A. B. (2016) TNFalpha-stimulated gene-6 (TSG6) activates macrophage phenotype transition to prevent inflammatory lung injury, *Proceedings of the National Academy of Sciences of the United States of America.* **113**, E8151-E8158.
20. Bredholt, G., Mannelqvist, M., Stefansson, I. M., Birkeland, E., Bo, T. H., Oyan, A. M., Trovik, J., Kalland, K. H., Jonassen, I., Salvesen, H. B., Wik, E. & Akslen, L. A. (2015) Tumor necrosis is an important hallmark of aggressive endometrial cancer and associates with hypoxia, angiogenesis and inflammation responses, *Oncotarget.* **6**, 39676-91.
21. Swinson, D. E., Jones, J. L., Richardson, D., Cox, G., Edwards, J. G. & O'Byrne, K. J. (2002) Tumour necrosis is an independent prognostic marker in non-small cell lung cancer: correlation with biological variables, *Lung cancer.* **37**, 235-40.
22. Leek, R. D., Landers, R. J., Harris, A. L. & Lewis, C. E. (1999) Necrosis correlates with high vascular density and focal macrophage infiltration in invasive carcinoma of the breast, *British journal of cancer.* **79**, 991-5.
23. Deryugina, E. I. & Quigley, J. P. (2015) Tumor angiogenesis: MMP-mediated induction of intravasation- and metastasis-sustaining neovasculature, *Matrix biology : journal of the International Society for Matrix Biology.* **44-46**, 94-112.
24. Day, A. J. & de la Motte, C. A. (2005) Hyaluronan cross-linking: a protective mechanism in inflammation?, *Trends in immunology.* **26**, 637-43.

25. Zhang, S., He, H., Day, A. J. & Tseng, S. C. (2012) Constitutive expression of inter-alpha-inhibitor (IalphaI) family proteins and tumor necrosis factor-stimulated gene-6 (TSG-6) by human amniotic membrane epithelial and stromal cells supporting formation of the heavy chain-hyaluronan (HC-HA) complex, *The Journal of biological chemistry.* **287**, 12433-44.
26. Shrimali, R. K., Yu, Z., Theoret, M. R., Chinnasamy, D., Restifo, N. P. & Rosenberg, S. A. (2010) Antiangiogenic agents can increase lymphocyte infiltration into tumor and enhance the effectiveness of adoptive immunotherapy of cancer, *Cancer research.* **70**, 6171-80.
27. Jiang, D., Liang, J. & Noble, P. W. (2011) Hyaluronan as an immune regulator in human diseases, *Physiological reviews.* **91**, 221-64.
28. Mytar, B., Woloszyn, M., Szatanek, R., Baj-Krzyworzeka, M., Siedlar, M., Ruggiero, I., Wieckiewicz, J. & Zembala, M. (2003) Tumor cell-induced deactivation of human monocytes, *Journal of leukocyte biology.* **74**, 1094-101.
29. del Fresno, C., Otero, K., Gomez-Garcia, L., Gonzalez-Leon, M. C., Soler-Ranger, L., Fuentes-Prior, P., Escoll, P., Baos, R., Caveda, L., Garcia, F., Arnalich, F. & Lopez-Collazo, E. (2005) Tumor cells deactivate human monocytes by up-regulating IL-1 receptor associated kinase-M expression via CD44 and TLR4, *Journal of immunology.* **174**, 3032-40.
30. Zhang, G., Guo, L., Yang, C., Liu, Y., He, Y., Du, Y., Wang, W. & Gao, F. (2016) A novel role of breast cancer-derived hyaluronan on inducement of M2-like tumor-associated macrophages formation, *Oncoimmunology.* **5**, e1172154.
31. Bertani, F. R., Mozetic, P., Fioramonti, M., Iuliani, M., Ribelli, G., Pantano, F., Santini, D., Tonini, G., Trombetta, M., Businaro, L., Selci, S. & Rainer, A. (2017) Classification of M1/M2-polarized human macrophages by label-free hyperspectral reflectance confocal microscopy and multivariate analysis, *Scientific reports.* **7**, 8965.
32. Dirkx, A. E., Oude Egbrink, M. G., Wagstaff, J. & Griffioen, A. W. (2006) Monocyte/macrophage infiltration in tumors: modulators of angiogenesis, *Journal of leukocyte biology.* **80**, 1183-96.
33. Xu, J., Rodriguez, D., Petitclerc, E., Kim, J. J., Hangai, M., Moon, Y. S., Davis, G. E. & Brooks, P. C. (2001) Proteolytic exposure of a cryptic site within collagen type IV is required for angiogenesis and tumor growth in vivo, *The Journal of cell biology.* **154**, 1069-79.
34. Takahashi, K., Eto, H. & Tanabe, K. K. (1999) Involvement of CD44 in matrix metalloproteinase-2 regulation in human melanoma cells, *International journal of cancer.* **80**, 387-95.
35. Zhong, X., Chen, B. & Yang, Z. (2018) The Role of Tumor-Associated Macrophages in Colorectal Carcinoma Progression, *Cellular physiology and biochemistry : international journal of experimental cellular physiology, biochemistry, and pharmacology.* **45**, 356-365.
36. Choi, J., Gyamfi, J., Jang, H. & Koo, J. S. (2018) The role of tumor-associated macrophage in breast cancer biology, *Histology and histopathology.* **33**, 133-145.
37. Wahl, L. M. & Smith, P. D. (2001) Isolation of Monocyte/Macrophage Populations in *Current Protocols in Immunology*, John Wiley & Sons, Inc.
38. Fujimoto, T., Savani, R. C., Watari, M., Day, A. J. & Strauss, J. F., 3rd (2002) Induction of the hyaluronic acid-binding protein, tumor necrosis factor-stimulated gene-6, in cervical smooth muscle cells by tumor necrosis factor-alpha and prostaglandin E(2), *The American journal of pathology.* **160**, 1495-502.
39. Alaniz, L., Garcia, M., Cabrera, P., Arnaiz, M., Cavaliere, V., Blanco, G., Alvarez, E. & Hajos, S. (2004) Modulation of matrix metalloproteinase-9 activity by hyaluronan is dependent on NF-kappaB activity in lymphoma cell lines with dissimilar invasive behavior, *Biochemical and biophysical research communications.* **324**, 736-43.

40. Pasarica, M., Sereda, O. R., Redman, L. M., Albarado, D. C., Hymel, D. T., Roan, L. E., Rood, J. C., Burk, D. H. & Smith, S. R. (2009) Reduced adipose tissue oxygenation in human obesity: evidence for rarefaction, macrophage chemotaxis, and inflammation without an angiogenic response, *Diabetes.* **58**, 718-25.

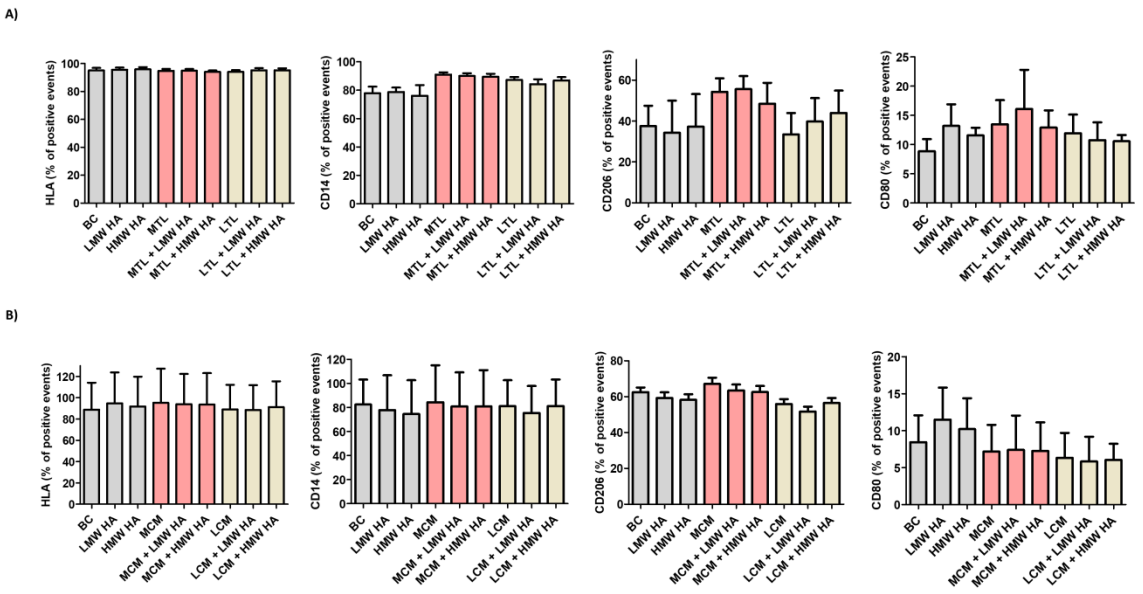

Figure 1. Characterization of Mo/MØ by Flow Cytometry. Mo/MØ culture treatments stained with mAbs anti A) HLA, B) CD14, C) CD80 and D) CD206. Mo/MØ were gated and the co-expression of the markers were analyzed. Data are expressed as mean percentage ± SEM from three independent experiments. Data was analyzed through one- way ANOVA analysis. BC = basal control; LMW HA = low molecular weight hyaluronan; HMW HA = high molecular weight hyaluronan; MTL = MDA-MB-231 tumor cell lysate; LTL = LoVo tumor cell lysate.

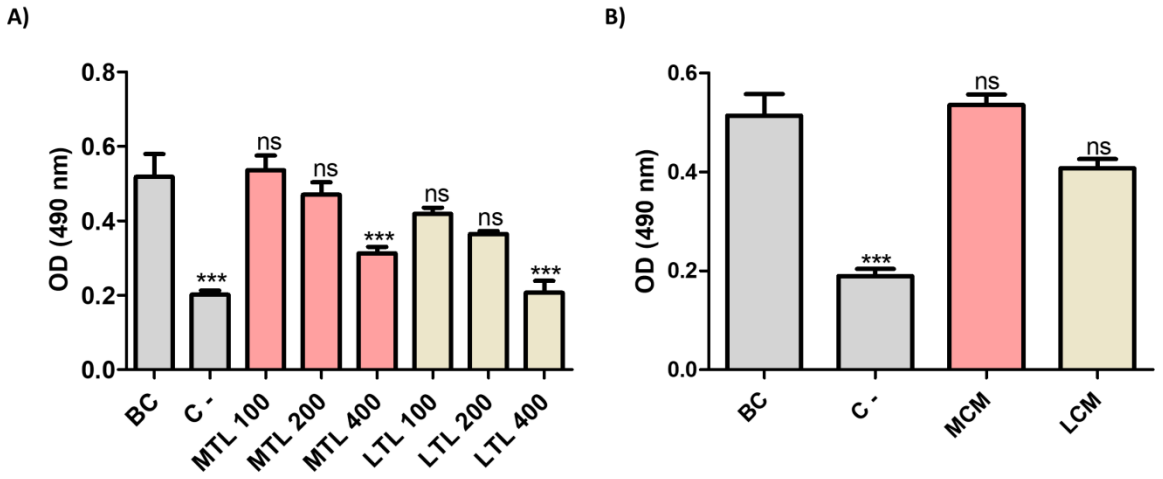

Figure 2. Cell Viability. Mo/MØ were cultured with A) different concentrations of MTL or LTL and B) MCM or LCM, and cell viability was measured using MTS assay. Data are expressed as optical density (OD) mean ± SEM from three independent experiments. (***) $p<0.001$ vs. control, one- way ANOVA analysis. C - = negative control, cell death was induced; OD = optical density.

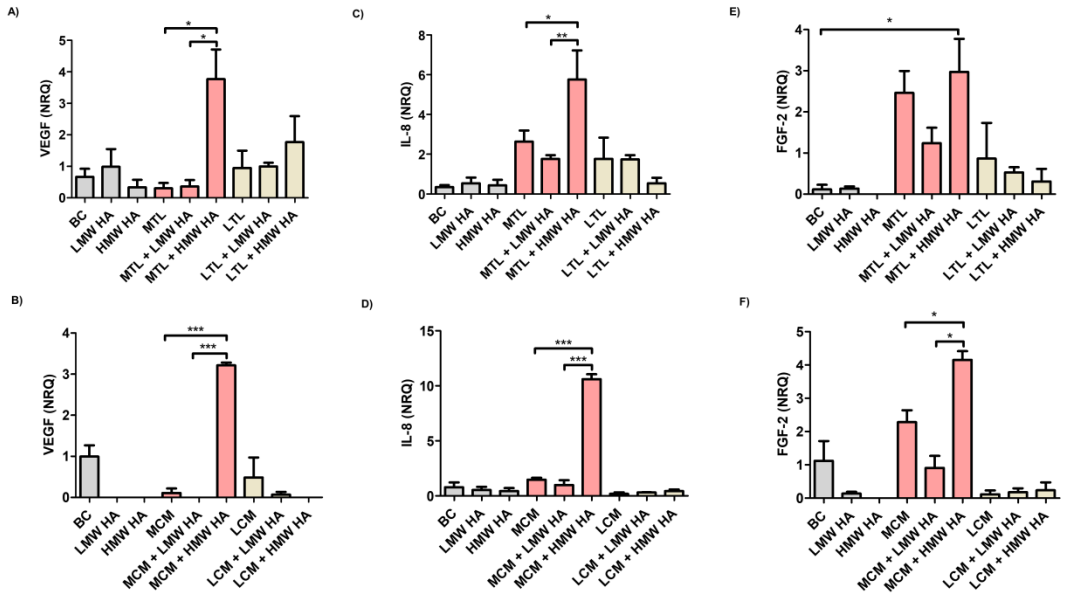

Figure 3. ***In vitro*** **angiogenesis in Mo/MØ treated with HA.** (A and B) VEGF, (C and D) IL-8 and (E and F) FGF-2 mRNA expression levels were measured by RT-qPCR in Mo/MØ. Data are expressed as normalized relative quantities (NRQ) mean ± SEM, from three independent experiments. (*) $p<0.05$, (**) $p<0.01$ and (***) $p<0.001$, one- way ANOVA analysis. BC = basal control; LMW HA = low molecular weight hyaluronan; HMW HA = high molecular weight hyaluronan; MTL = MDA –MB 231 tumor cell lysate; MCM= MDA – MB 231; conditioned media LTL = LoVo tumor cell lysate; LCM: LoVo conditioned media.

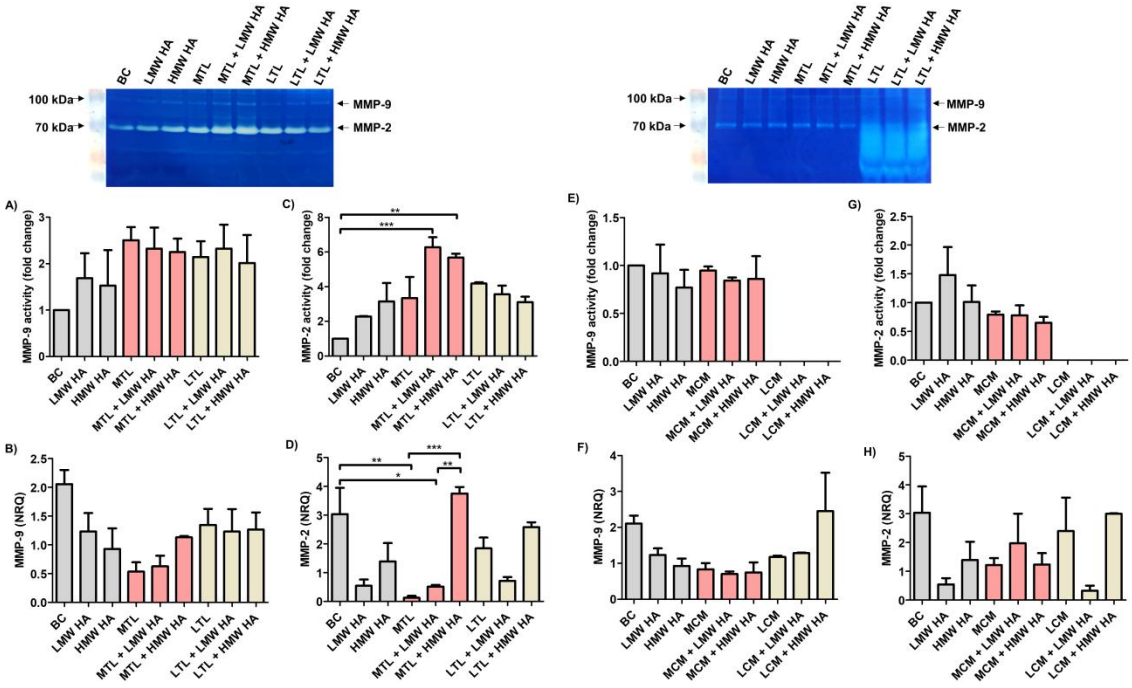

Figure 4. MMPs activity and mRNA levels in Mo/MØ treated with HA. (A; C; E and G). MMPs activity was analyzed by gelatin zymography. MMP-2 activity in Mo/MØ supernatants treated with TL (C) or CM (G) and HA (LWW and HMW). MMP-9 activity in Mo/MØ supernatants treated with TL (A) or CM (E) and HA (LWW and HMW). The activity was quantified by densitometry and relative activity was obtained by normalizing values to untreated samples. Data are expressed as fold change mean ± SEM and correspond to three independent experiments. (B; D; F and H) mRNA expression levels measured by RT-qPCR. MMP-2 mRNA levels in Mo/MØ supernatants treated with TL (D) or CM (H) and HA (LWW and HMW) and MMP-9 mRNA levels in Mo/MØ supernatants treated with TL (B) or CM (F) and HA (LWW and HMW) Data are expressed as normalized relative quantities (NRQ) mean ± SEM, from three independent experiments.
(*) $p<0.05$, (**) $p<0.01$ and (***) $p<0.001$, one- way ANOVA analysis. BC = basal control; LMW HA = low molecular weight hyaluronan; HMW HA = high molecular weight hyaluronan; MTL = MDA –MB 231 tumor cell lysate; MCM= MDA –MB 231; conditioned media LTL = LoVo tumor cell lysate; LCM: LoVo conditioned media.

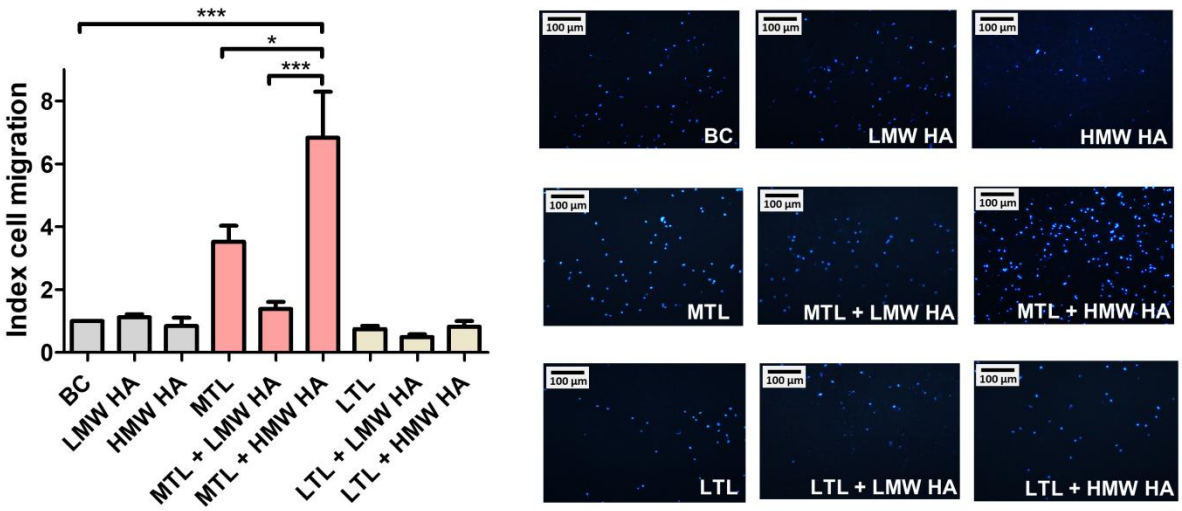

Figure 5. Endothelial cells migration towards Mo/MØ supernatants treated with HA. Results are expressed as an index of cell migration with respect to nontreated BC ± SEM from three representative visual fields. Results are representative of three independent experiments. (*) $p<0.05$ and (***) $p<0.001$, one- way ANOVA analysis. BC = basal control. LMW HA = low molecular weight hyaluronan; HMW HA = high molecular weight hyaluronan; MTL = MDA –MB 231 tumor cell lysate; LTL = LoVo tumor cell lysate.

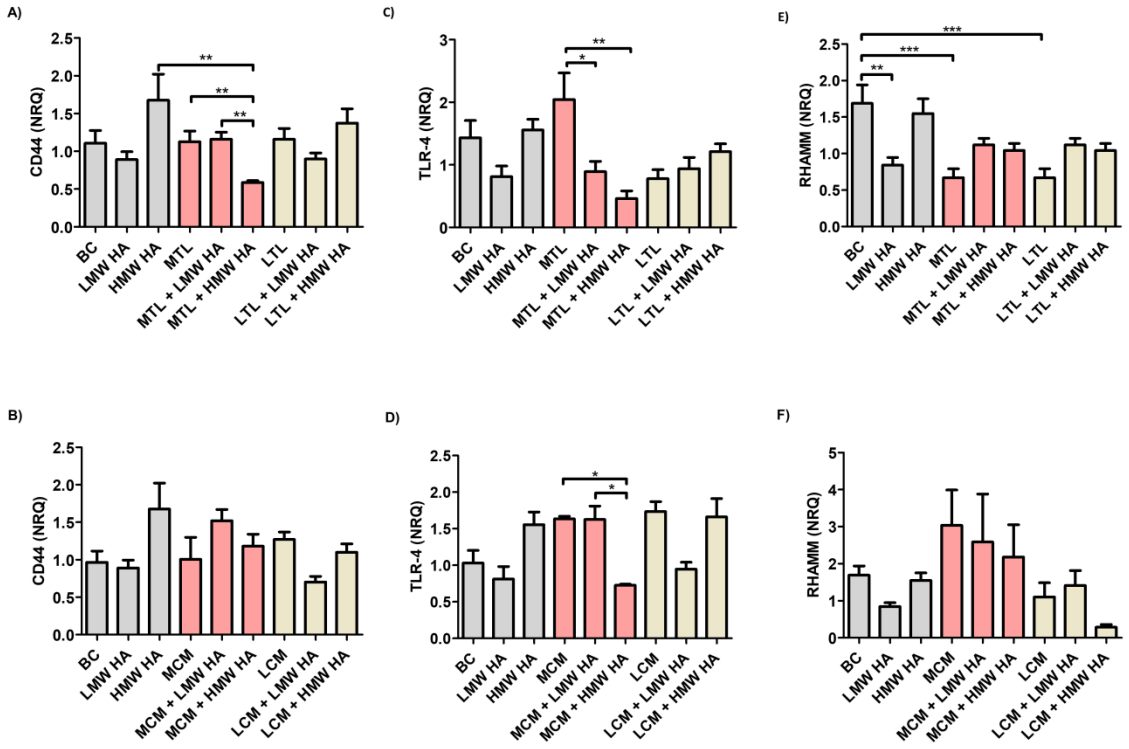

Figure 6. HA receptors mRNA levels in Mo/MØ treated with HA. (A-F) CD44, TLR-4, RHAMM mRNA expression levels measured by RT-qPCR mRNA levels measured by RT-qPCR in Mo/MØ treated with TL (A; C and E) or CM (B; D and F) and HA (LWW and HMW**).** Data are expressed as normalized relative quantities (NRQ) mean ± SEM, from four independent experiments. (*) $p<0.05$, (**) $p<0.01$ and (***) $p<0.001$, one- way ANOVA analysis. BC = basal control; LMW HA = low molecular weight hyaluronan; HMW HA = high molecular weight hyaluronan; MTL = MDA –MB 231 tumor cell lysate; MCM= MDA –MB 231; conditioned media LTL = LoVo tumor cell lysate; LCM: LoVo conditioned media.

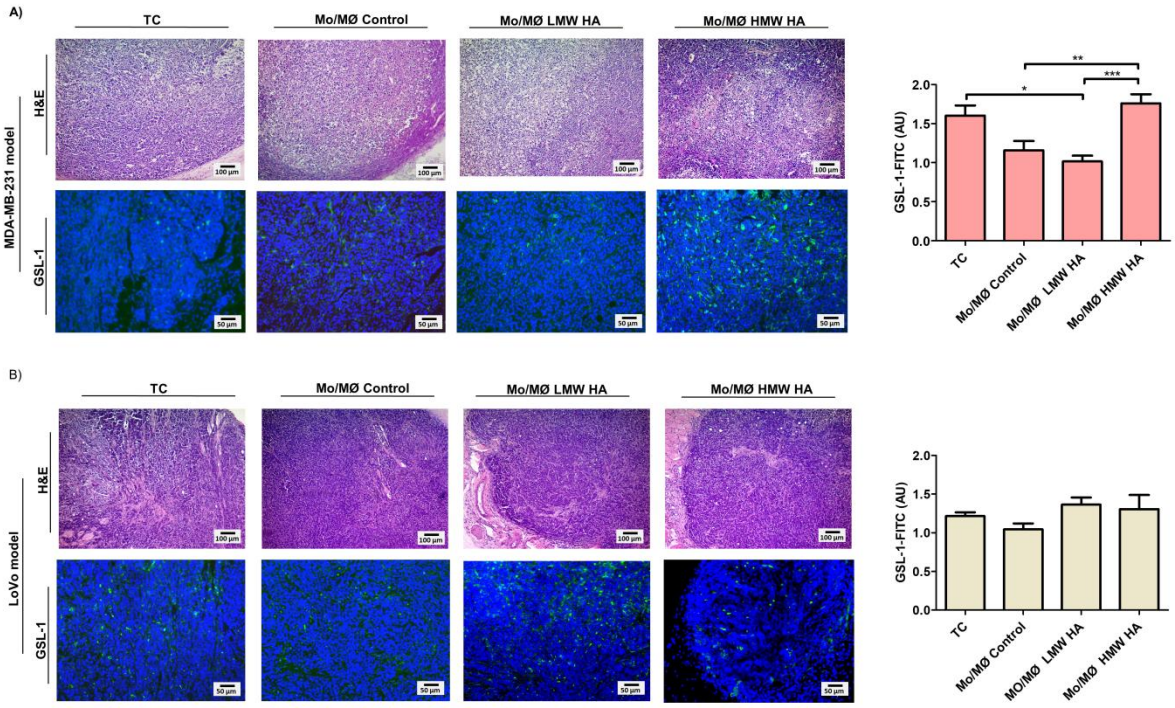

Figure 7. *In vivo* angiogenesis in cancer xenograft model. (A) MDA-MB-231 model and (B) LoVo model. H&E: tumors were fixed and stained with hematoxylin/eosin. GSL-1: quantification of GSL-1-FITC (binds specifically to endothelial cells) by fluorescence microscopy in tumor sections of breast cancer xenograft model. Nude mice were inoculated with MDA-MB 231 or LoVo and at day 9 tumors with a similar volume where inoculated with MO/MØ previously treated or not with LMW or HMW HA. Tumors were fixed and stained with GSL1-FICT (green, endothelial cells) and DAPI (blue, nuclei). Bars represent the average of GSL-1-FITC+/field ± SEM from ten representative visual fields. (*) $p<0.05$, (**) $p<0.01$ and (***) $P<0.001$, one- way ANOVA analysis. TC = Tumor Control; Mo/MØ = monocytes/ macrophages; LMW HA = low molecular weight hyaluronan; HMW HA = high molecular weight hyaluronan.

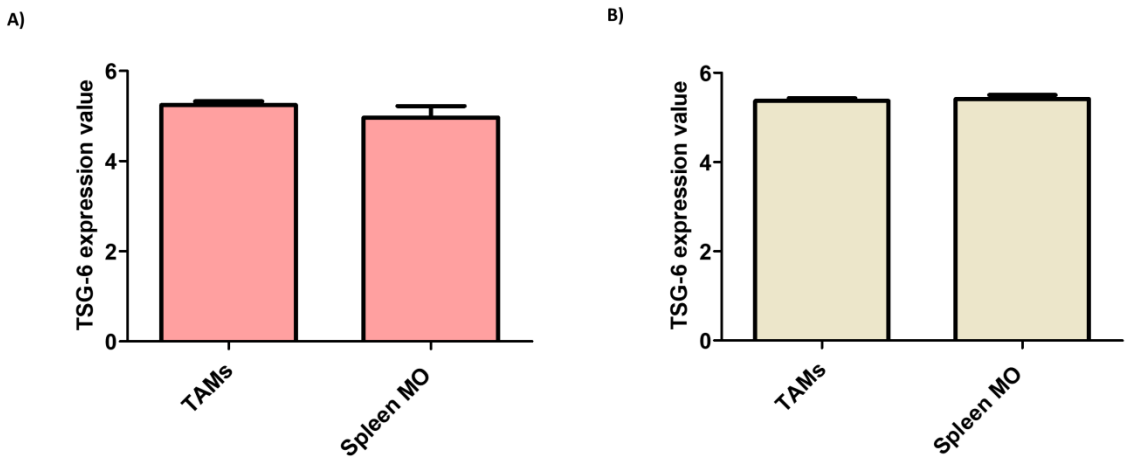

Figure 8. Microarray datasets GSE18404 (breast carcinoma) and GSE67953 (colorectal carcinoma) were used for comparing differential TSG-6 expression levels in TAMs and spleen MO. In each dataset, NCBI GEO2R tool was used to analyze TSG-6 levels.

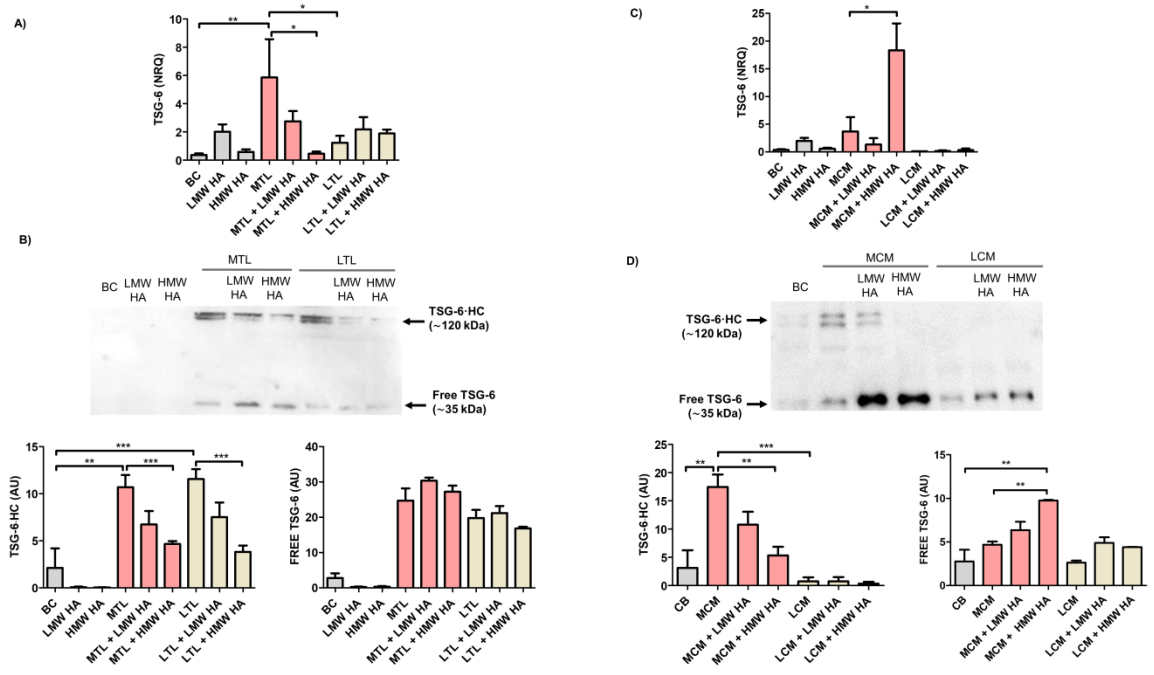

Figure 9. TSG-6 mRNA and protein levels in Mo/MØ treated with HA. (A and C) TSG-6 mRNA expression levels were measured by RT-qPCR in Mo/MØ treated with TL (A) or CM (C) and HA (LWW and HMW). Data are expressed as normalized relative quantities (NRQ) mean ± SEM, from three independent experiments. (B and D) TSG-6 protein levels were measured by western blot in Mo/MØ supernatants MØ treated with TL (B) or CM (D) and HA (LWW and HMW). TSG-6· HC (~120 kDa) right panel; Free TSG-6 (~35 kDa) left panel. Protein levels were quantified by densitometry from four independent experiments. (*) $p<0.05$, (**) $p<0.01$ and (***) $p<0.001$, one- way ANOVA analysis. BC = basal control; LMW HA = low molecular weight hyaluronan; HMW HA = high molecular weight hyaluronan; MTL = MDA –MB 231 tumor cell lysate; MCM= MDA –MB 231; conditioned media LTL = LoVo tumor cell lysate; LCM: LoVo conditioned media.

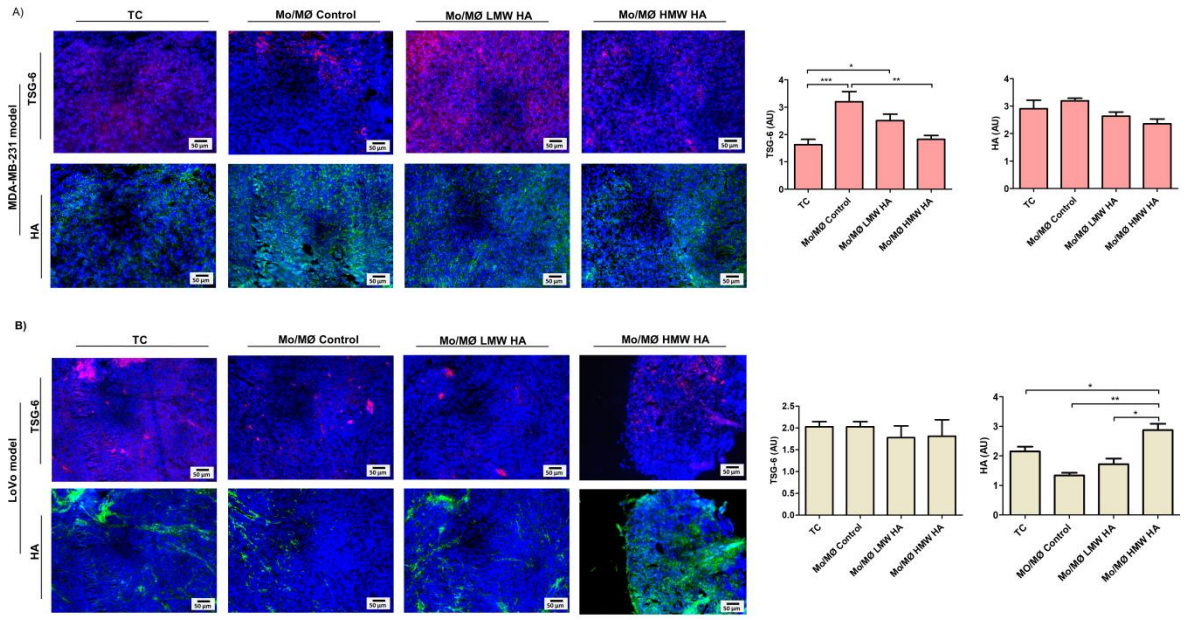

Figure 10. TSG-6 and HA immunostaining in cancer xenograft model. (A) MDA-MB-231 model, (B) LoVo model. Tumors sections were stained with: TSG6 and anti-rabbit conjugated with Texas Red (red, TSG-6); HA binding protein biotinylated and streptavidin-FITC (green, total HA); and DAPI (blue, nuclei). Bars represent the average of TSG-6+ or HA+/field ± SEM from ten representative visual fields. (*) $p<0.05$, (**) $p<0.01$ and (***) $P<0.001$, one- way ANOVA analysis. TC = Tumor Control; Mo/ MØ = monocytes/macrophages; LMW HA = low molecular weight hyaluronan; HMW HA = high molecular weight hyaluronan.

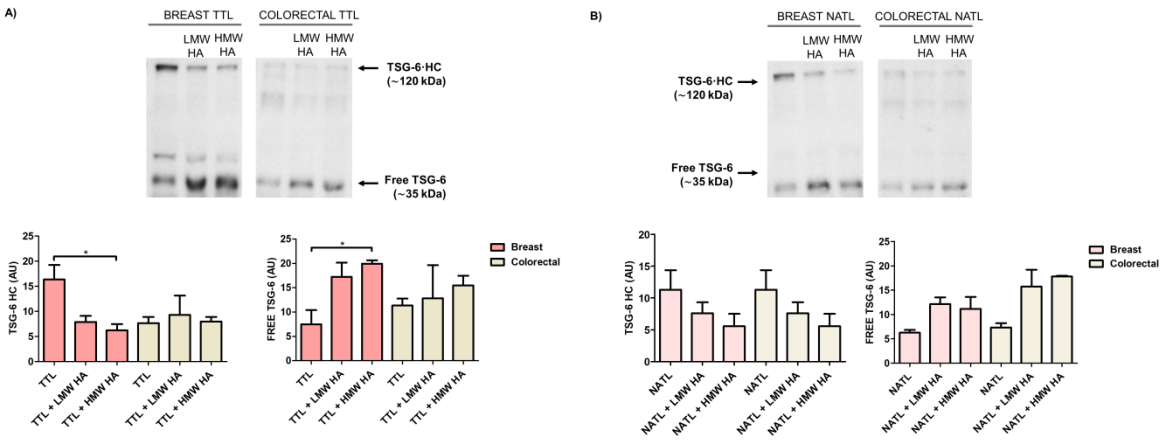

Figure 11. TSG-6 protein levels in Mo/MØ treated with HA derived from patients (breast and colorectal cancer). (A) TSG-6 protein levels were measured by western blot in Mo/MØ supernatants MØ treated with TL derived from breast or colorectal tumor tissue and HA (LWW and HMW). (B) TSG-6 protein levels were measured by western blot in Mo/MØ supernatants MØ treated with NATL derived from breast or colorectal normal tissue adjacent to the tumor. TSG-6· HC (~120 kDa) right panel; Free TSG-6 (~35 kDa) left panel. Protein levels were quantified by densitometry and expressed as arbitrary units (AU) mean ± SEM, from four independent experiments. (*) $p<0.05$, one- way ANOVA analysis. BC = basal control; LMW HA = low molecular weight hyaluronan; HMW HA = high molecular weight hyaluronan; TTL = tumor tissue lysate; NATL= normal tissue adjacent to the tumor lysate.